

# A Flow-Guided Mutual Attention Network for Video-Based Person Re-Identification

Madhu Kiran<sup>a</sup>, Amran Bhuiyan<sup>a</sup>, Louis-Antoine Blais-Morin<sup>b</sup>, Mehrsan Javan<sup>c</sup>, Ismail Ben Ayed<sup>a</sup>, Eric Granger<sup>a</sup>

<sup>a</sup> Laboratoire d'imagerie, de vision et d'intelligence artificielle, École de technologie supérieure, Montreal, Canada

<sup>b</sup> Genetec Inc., Montreal Canada

<sup>c</sup> Sportlogiq Inc., Montreal Canada

mkiran@livia.etsmtl.ca, amran.apece@gmail.com

lablaismorn@genetec.com, mehrsan@gmail.com

Ismail.BenAyed@etsmtl.ca, eric.granger@etsmtl.ca

## Abstract

*Person Re-Identification (ReID) is a challenging problem in many video analytics and surveillance applications, where a person's identity must be associated across a distributed non-overlapping network of cameras. Video-based person ReID has recently gained much interest because it allows capturing discriminant spatio-temporal information from video clips that is unavailable for image-based ReID. Despite recent advances, deep learning (DL) models for video ReID often fail to leverage this information to improve the robustness of feature representations. In this paper, the motion pattern of a person is explored as an additional cue for ReID. In particular, a flow-guided Mutual Attention network is proposed for fusion of image and optical flow sequences using any 2D-CNN backbone, allowing to encode temporal information along with spatial appearance information. Our Mutual Attention network relies on the joint spatial attention between image and optical flow features maps to activate a common set of salient features across them. In addition to flow-guided attention, we introduce a method to aggregate features from longer input streams for better video sequence-level representation. Our extensive experiments on three challenging video ReID datasets indicate that using the proposed Mutual Attention network allows to improve recognition accuracy considerably with respect to conventional gated-attention networks, and state-of-the-art methods for video-based person ReID.*

## 1. Introduction

Person Re-Identification (ReID) refers to the problem of associating individuals over a set of non-overlapping camera views. It is one of the key object recognition tasks, that has recently drawn a significant attention due to its

wide range of applications in monitoring and surveillance, e.g., multi-camera target tracking, pedestrian tracking in autonomous driving, access control in biometrics, search and retrieval in video surveillance, and human-computer interaction communities. Despite the recent progress with deep learning (DL) models, person re-identification remains a challenging task due to the non-rigid structure of the human body, the variability of capture conditions (e.g., illumination, blur), occlusions and background clutter.

ReID systems can apply in image-based and video-based settings. State-of-the-art [1, 2, 3, 4, 14, 33, 47, 35, 48] approaches on image-based setting seek to associate still images of individuals over a set of non-overlapping cameras. In case of video based ReID where input video tracklets of an individual are matched against a gallery of tracklet representations, captured with different non-overlapping cameras. A tracklet corresponds to a sequence of bounding boxes that were captured over time for a same person in a camera viewpoint, and are obtained using a person detector and tracker. Compared to image data, video data provides richer source of information about persons' appearance along with motion information that notably capture persons' body layouts. Thus, video-based approaches allow to exploit spatio-temporal information (appearance and motion) for discriminative feature representation.

As illustrated in Figure 1, state-of-the-art approaches for video-based person ReID typically learn global features in an end-to-end fashion, through various temporal feature aggregation techniques [16, 17, 19, 31, 44]. From this figure, the query input to the feature extractor is a video clip(set of bounding boxes extracted from a tracklet) of  $N$  frames long. A single feature vector is extracted by aggregating features from each frame in the query video clip. This is then compared with a gallery containing  $n$  identities which is set of aggregated feature representations of clips from previously-

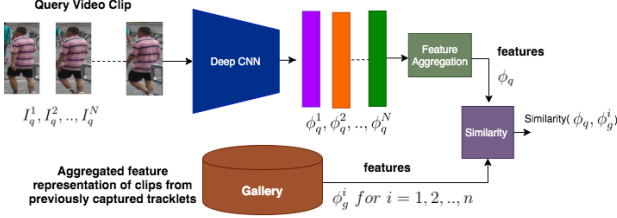


Figure 1. Block diagram of a generic DL model specialized for video-based person ReID. Each query video clip from a non-overlapping camera is input to a backbone CNN to produce a set of features embeddings, one per image. The features are then aggregated to produce a single feature representation for the clip, which is then matched against clip representations stored in the gallery.

captured tracklets.

Given a video clip (fixed size set of bounding boxes extracted from a tracklet), the feature extractor (CNN backbone) produces image-level features, while the feature aggregator generates a single feature representation at the clip level, using either average pooling, weighted addition, max pooling, recurrent NNs, etc. [16] in the temporal domain. Although these aggregation approaches enable to incorporate diverse tracklet information for matching, and can achieve a higher level of accuracy that image-based approaches, they often fail to efficiently capture temporal information which could propagate as salient features throughout the video sequence. Additionally, the performance of state-of-the-art methods decline as the length of video clips grows beyond 4 or 6 frames [16, 44].

Optical flow stream has been previously used as additional stream of input captures the motion dynamics of a walking person in a video stream. At the same time, as shown in Fig. 2, visual appearance of optical flow for a walking or moving person is very close to the silhouette of the person often suppressing the background static objects. This has a potential to be able to be used as a mask on appearance stream to highlight common saliency between frames. The potential silhouette produce by optical flow together with it highlighting common saliency across frames can therefore be a good source of spatio-temporal attention.

Fig. 2 shows that the flow features are coarse representation of semantic information of moving objects. Unlike action recognition which depends heavily on motion features, ReID is more dependent on appearance features. Hence, there is a scope to combine the strengths of optical flow and appearance (video stream) features for ReID. Previous attempts to include optical flow information into ReID systems [12, 32, 49] focused on integrating this information as an additional input in the network with some kind of integration into the main features later. This is not effective because optical flow only represents coarse semantic features of moving objects (different from the image stream), and not image-like appearance information. Moreover the model in [12] is related to a two-stream network proposed



Figure 2. Example of a sequence of bounding boxes images from the MARS dataset (top row), and its corresponding dense optical flow map (bottom row). The common saliency in the sequence can be observed from the optical flow map.

in [39] that incorporates motion and appearance feature for action recognition. Two-stream networks that are effective for action recognition are less effective for ReID [12].

Given the aforementioned justification, in this work the correlation between the visual appearances across motion and appearance stream along with their individual contribution to motion dynamics are considered. In order to capture long term spatial information and temporal dynamics in a video clip, a method to aggregate features from longer sequence effectively is presented. This has not been explored in the literature for video person-ReID, thereby undermining the global saliency in the feature representation by using optical flow for both appearance and motion information.

In this paper, DL model for flow-guided attention is introduced for video-based person ReID to enable joint spatial attention between input temporal(optical flow) and image stream (video sequence). The proposed Mutual Attention network enables to jointly learn a feature embedding that incorporates relevant spatial information from human appearance, along with their motion information, from both appearance stream (images) and motion stream (optical flow). The Mutual Attention network includes both optical flow stream and image stream for ReID and leverages the mutual appearance and motion information.

We also propose a feature aggregation method to capture long-range temporal relationship by being able to aggregate information from longer video tracklets or sequences. Unlike prior work in literature where feature aggregation is achieved by pooling or temporal attention from image feature, the proposed Mutual Attention network relies on a weighted feature addition method over images in a sequence to produce a single feature descriptor using both optical flow and image feature information. During feature aggregation, a reference frame from each tracklet is selected based on maximum activation from both the streams, and weights are assigned for individual features using image and flow feature information. Attention is enabled from optical

flow in both spatial and temporal domain to extract discriminant features for ReID.

Performance of the proposed flow-guided attention network is evaluated and compared on the challenging MARS, Duke-MTMC datasets and ILIDS-Vid dataset for video-based person ReID. Experimental results show that both improve accuracy and can outperform the state-of-the-art approaches. Results also indicate the capability for higher accurate predictions by using longer video clips to capture multiple appearance variations.

## 2. Related Work

The section provides background on DL models for spatio-temporal recognition, optical flow, and attention mechanisms as they relate to person ReID.

**a) Image-Based Person-ReID:** The idea of using CNNs for ReID stems from Siamese Network [5], which involves two sub-networks with shared weights, and is suitable for finding the pair-wise similarity between query and reference images. It has first been used in [54] that employs three Siamese sub-networks for deep feature learning. Since then many authors focus on designing various DL architectures to learn discriminative feature embedding. Most of these deep-architecture based ReID [1, 10, 50, 9, 9, 28] approaches introduce an end-to-end ReID framework, where both feature embedding and metric learning have been investigated as a joint learning problem. In [1, 50], a new layer is proposed to capture the local relationship between two images, which helps modeling pose and viewpoint variations in cross-view pedestrian images. Recent ReID approaches [43, 45, 58, 56, 34, 57, 37, 47, 2] rely on incorporating contextual information into the base deep ReID model, where local and global feature representations are combined to improve accuracy. A few attention-based approaches for deep re-ID [23, 57, 43] address misalignment challenges by incorporating a regional attention sub-network into a base re-ID model. A thorough review of state-of-the-art on architecture-based approaches underscores the importance of considering local representations, e.g., by dividing the image into soft stripes [47] or by pose-based part representation [43, 45, 58, 56, 34, 57, 37]. Although these methods have achieved considerable performance improvements, they fail to incorporate temporal information due to their image-based setting.

**b) Video-Based Person-ReID:** Video ReID has recently attracted some interest since temporal information allows dealing with ambiguities such as occlusion and background noise [16, 17, 44, 19, 31]. An important problem in video-based ReID is the task of aggregating the image level features to obtain one single composite feature or descriptor for a video sequence. [16] have approached this problem by frame level feature extraction and temporal fusion by using recurrent NNs (RNNs), average pooling, and tempo-

ral attention (based on image features). Average Pooling in temporal dimension can be viewed as summing the features of the sequence by giving equal normalised weights to them. Average pooling of image instance features from a given sequence have proved to be useful in most of the cases, even compared to other DL model based on RNNs or 3D-CNN [16]. 3DCNN has been experimented in [16, 25] but have not been very effective in summarising video sequence for reID. But there could be certain case of individual image in a sequence such that they either have higher noise content or the appearance in the image does not contribute much to an individual's identity, then these become the debatable cases for Average Pooling.

**c) Attention Mechanisms:** Attention can be interpreted as a means of biasing the allocation of available computational resources towards the most informative components of a signal [20]. A mask guided attention mechanism has been proposed in [40], where a binary body mask is used in conjunction with the corresponding person image to reduce background clutter. Somewhat similar to [40], co-segmentation networks have achieved significant improvements in ReID accuracy over the baseline by connecting a new COSAM module between different layers of a deep feature extraction network [44]. Co-Segmentation allows extracting common saliency between images, and using this information for both spatial- and channel-wise attention. Other related work for attention in video ReID, [7] attention is employed in both temporal and spatial domain. Video stream has been taken advantage of by [41] by extracting complementary region based feature by from different frames to obtain informative features as a whole.

**d) Optical Flow as Temporal Stream:** It often serves as a good approximation of the true physical motion projected onto the image plane [49]. Optical flow has been employed for temporal information fusion in [12, 32], in a two stream Siamese Network with a weighted cost function to combine the information from both the streams. It uses a CNN that accepts both optical flow and color channels as input, and a recurrent layer to exploit temporal relations. Its important to note that prior to [12], [39] have used two stream networks but for action recognition. Two stream networks on their own are useful in action recognition as impact of motion cues in action recognition are higher in action recognition than that of ReID [12]. Therefore there is a necessity to use optical flow in a way that it can be leveraged for appearance related task. However, traditional two-stream networks are unable to exploit a critical component in re-id i.e appearance across both optical flow and image stream together. Similar to our motivation for using optical flow for appearance along with motion has been discussed in [30]. Similar to our work, motivation for considering long term temporal relationship has been discussed in [11].

It can be summarised from the above that, as discussed in

[44], [38],[40] and [38], various saliency feature enhancement methods have been attempted, and in most cases, they help improve the overall performance. Optical flow typically encodes motion information in contrast to appearance information, and hence there is scope to explore enhancing appearance information from motion and vice-versa. Also, based on [11] and [30], highlight the advantages of long term temporal information and appearance across both optical flow and image stream together.

### 3. Proposed Mutual Attention Network

Given an input video clip (set of consecutive bounding boxes extracted from a tracklet) represented by  $\mathbf{I}_c^1, \mathbf{I}_c^2, \dots, \mathbf{I}_c^n$  and corresponding optical flow estimations  $\mathbf{F}_c^1, \mathbf{F}_c^2, \dots, \mathbf{F}_c^n$  where  $c$  indicates the Identity of the video clip of length  $n$ , our objective is to extract a discriminative feature vector  $\phi_c$  for ReID.

A new model for flow guided attention – Mutual Attention network is proposed. It learns spatial-temporal attention from optical flow thereby focusing on common salient features of a given person during its motion across consecutive frames of a given video clip. Although a two stream Siamese network has been proposed in [12], they have included optical flow as an input for re-identification, and do not exploit the full potential of this information. Hence as discussed earlier, the motivation behind this work is to take advantage of visual appearance of both spatial and temporal stream i.e image and optical flow stream by producing a correlation map between them in the feature space. This correlation map is used as attention on both the input streams. The temporal information in both the streams is enhanced by enabling the use of longer video and optical flow clips with our proposed feature aggregation method.

Therefore our Mutual Attention network includes both optical flow and image streams which attend each other to obtain Mutual Attention and also to combine the features to yield a single feature representation per input pair of image and optical flow clip.

This is illustrated in Fig. 3, where the network accepts two streams of input (optical flow and image sequences). At the last layer of the network, the features from the two streams are concatenated after feature aggregation in the temporal domain. While the image stream helps in ReID by focusing on the appearance of the person, optical flow stream helps by capturing motion pattern of a given person. We propose to achieve feature aggregation to produce a feature vector by weighted addition. Our proposed method handles generation of weights that indicate the importance of individual image feature in producing a single video feature leveraging upon mutual attention.

In contrast to the previous method for flow guided attention mention above, we propose to produce cross-stream attention or Mutual attention between the optical flow stream

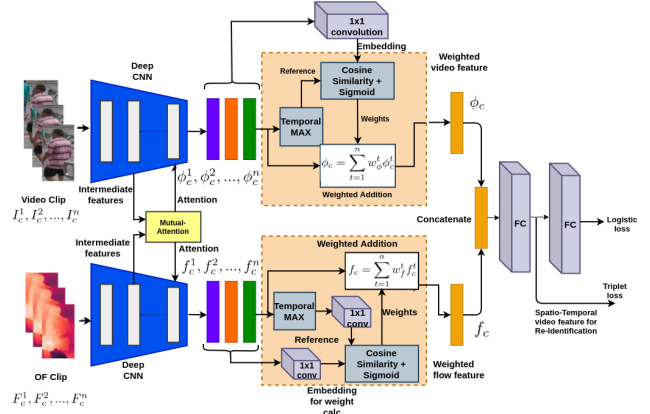


Figure 3. Our proposed Mutual Attention network. The input to the system is a video clip and corresponding flow maps. The features extracted from each other apply Mutual Attention to each other. The network outputs a concatenated feature from both optical flow and image stream.

and image stream to boost areas in the feature space that have high activation across both the streams.

Given a video clip and corresponding flow maps, we extract the features  $\phi_c$  and  $f_c$  from the deep CNNs respectively. The expected output is a concatenated feature vector of both optical flow and image features to be used for ReID. Both the CNNs share common architecture but do not share the parameters. Let  $l$  be the intermediate layer of the  $k$ -layer deep CNN and let appearance CNN be represented by  $H_{app}$  and optical flow stream CNN by  $H_{flow}$  with a total number of  $k$  layers. With  $t = 1, 2, 3 \dots n$  we have:

$$\phi_c^t = H_{app}(\mathbf{I}_c^t), \quad f_c^t = H_{flow}(\mathbf{F}_c^t) \quad (1)$$

If features from layer  $l$  are expressed as  $\phi^l$ , then

$$\phi_c^{l,t} = H_{app,l}(\mathbf{I}_c^t), \quad f_c^{l,t} = H_{flow,l}(\mathbf{F}_c^t) \quad (2)$$

Both the features at layer  $l$  are of dimensions,  $N \times C \times I \times J$ , representing sequence length, channels, width, height respectively. The features are then passed through  $1 \times 1$  convolution with *Relu* activation to produce a map of size  $N \times 1 \times I \times J$  each. The correlation between the features is given by,

$$\rho = \zeta_{app}(\phi_c^{l,t}) \odot \zeta_{flow}(f_c^{l,t}) \quad (3)$$

In the Eq. 3,  $\zeta_{app}$  and  $\zeta_{flow}$  are the embeddings with  $1 \times 1$  convolution with *Relu* discussed above.  $\rho$  when activated by a sigmoid function forms the mutual attention map  $M_c^t$  between both the streams of input.

$$M_c^t = \frac{1}{1 + e^{-\rho}} \quad (4)$$

Finally, mutual attention is applied to the intermediate features  $\phi_c^{l,t}$  and  $f_c^{l,t}$  at the intermediate layer (by an element-wise multiplication of attention map with feature maps) to

obtain mutually attended appearance features  $\Psi_{app}$  and  $\Psi_{flow}$  to continue feature extraction continues in the remaining layers of the deep CNN to obtain final output features  $\phi_c^t$  and  $f_c^t$  for image and flow stream, respectively:

$$\Psi_{app_c}^t = \phi_c^{l,t} \odot M_c^t, \quad \Psi_{flow_c}^t = f_c^{l,t} \odot M_c^t \quad (5)$$

**Weighted Feature Addition.** We propose a method to aggregate image level features to obtain a single feature vector for a given video sequence particularly enabling to use longer video sequences. The appearance features and optical flow features are then concatenated to for ReID during inference, and to learn a classifier during training.

The output from image and optical flow stream CNNs generate  $\phi_c$  for a sequence  $c$  from instances  $\phi_c^1, \phi_c^2, \dots, \phi_c^n$  and  $f_c$  from  $f_c^1, f_c^2, \dots, f_c^n$ . The first task is to identify salient feature from a given sequence of features. In our case, a salient feature can be defined as the one that has maximum activation in both image and flow stream. Since the features have been attended by mutual attention, given a sequence, a max operation in the temporal domain for each of the sequence will identify the salient feature among the sequence. We hereafter will refer to this salient feature as reference frame denoted by  $\phi_c^{max}$  and  $f_c^{max}$ . In the next step an adaptive weight is generated for each of the features in the sequence based on how close each feature is with the reference feature. This is achieved by applying a cosine similarity between the reference feature and rest of the features in the sequence. The cosine similarity function is not applied directly on the features  $\phi_c^n$  and  $f_c^n$ . Instead a tiny embedding  $\epsilon(\cdot)$  is applied on the  $\phi_c^n, f_c^n$  and reference feature  $\phi_c^{max}, f_c^{max}$  to obtain embeddings  $\phi_\epsilon^n, f_\epsilon^n, \phi_\epsilon^{max}$  and  $f_\epsilon^{max}$ :

$$w_{app}^n = \exp \left( \frac{\phi_\epsilon^n \cdot \phi_\epsilon^{max}}{||\phi_\epsilon^n|| ||\phi_\epsilon^{max}||} \right) \quad (6)$$

$$w_{flow}^n = \exp \left( \frac{f_\epsilon^n \cdot f_\epsilon^{max}}{||f_\epsilon^n|| ||f_\epsilon^{max}||} \right) \quad (7)$$

$$\phi_c = \sum_{t=1}^n w_{app}^n \phi_c^n \quad (8)$$

From Eq. 6 and Eq. 7, feature aggregation weights are calculated for both image features and flow features respectively. The features are aggregated as per weighted aggregation Eq. 8 to form outputs  $\phi_c$  and when used with  $w_{flow}$  to obtain  $f_c$  which are aggregated video features for image and flow respectively. These two features are concatenated to form  $\phi_{cat}$  which is passed through a fully connected layer of size same as  $\phi_c$  to produce the final feature for classification or re-identification. The network is trained on logistic loss and Triplet loss similar to the method used in [44]. During testing the fully connected layer is removed and the

remainder of the network is used for feature extraction purpose and to match against those in gallery.

## 4. Experimental Methodology

In this section the experimental procedure is described to evaluate and compare the performance of proposed and reference feature aggregation methods. The implementation details describe the datasets, feature extraction models, parameters for flow feature estimation, optical flow estimation method, training and evaluation techniques. We first aim to compare the benefits of Mutual attention with two stream network against one stream network simple Gated Attention with optical flow. We also compare our feature aggregation model with other methods in Video ReID literature including averaging, temporal attention and Recurrent networks.

**Datasets.** Experiment are performed on 2 challenging and widely-used datasets for video-based person reID. MARS [42] dataset is one of the largest datasets for video Person-ReID. Another dataset commonly used in literature for evaluating video person ReID is Duke-MTMC [53], [36] dataset containing 702 identities and more than 2000 sequences for testing and training each. We also evaluate on ILIDS-VID [51] dataset, which has a total of 300 identities with videos across two cameras. One interesting point to be noted with ILIDS datasets is that the tracklets have been generated by hand annotation unlike detector based annotation in MARS dataset. This makes the bounding boxes well aligned in ILIDS-VID dataset enabling the optical flow estimation to be less noisy.

**Deep Feature Extraction.** We follow the overall system architecture in [16] (Baseline) and [44] (COSAM). They achieved state-of-the-art results on several ReID datasets. They have used ResNet50 for feature extraction. We propose to use ResNet50 and SE-ResNet 50 as our base networks to learn features invariant to cluttered background by attending with saliency map obtained from optical flow estimations. We have shown results with each of the networks as back end separately. The networks have been pre-trained on imagenet [13] dataset. We experiment at different layers of the ResNet50 to select the ideal location in the network to generate maximum attention with optical flow. To extract video level feature from instance level features, we compare our proposed weighted addition method with that of temporal Average Pooling (AP) and Temporal Attention (TA) based method as illustrated in [16] and [44]. The Shallow CNN in our experimental setup for gated attention is based on AlexNet and the sub-Network for weighted addition is a two layer MLP of size 2048 nodes in each layer.

**Optical Flow Estimation.** To estimate optical flow maps for a given sequence LiteFlowNet [22] model has been cho-

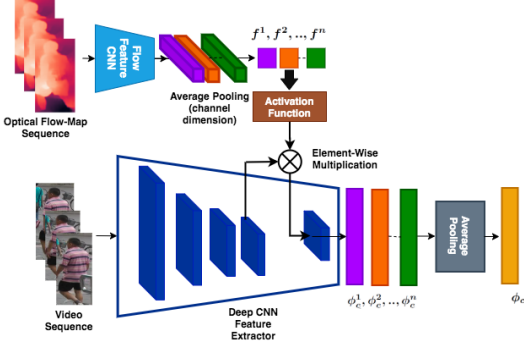


Figure 4. Our experimental setup for our baseline gated attention network. The system inputs a sequence of bounding boxed images and the corresponding optical flow maps from a given video clip. The features extracted from optical flow are pooled in channel dimension, and multiplied with intermediate layers of deep feature extraction after activation to obtain attended features for ReID. The network outputs a feature vector  $\phi_c$  per video clip.

sen as they are computationally efficient compared to other deep models along with obtaining state of the art performance. We have used the official implementation from the authors to produce flow maps for both MARS and DukeMTMC dataset. Hence for a given sequence, we input pairs of image  $I^{t-1}, I^t$  as input to the LiteFlowNet model to produce flow map  $F^{t-1}$ .

**Evaluation Measures.** During the training phase we learn the ReID task by training a classifier with identity labels from the single feature extracted for a sequence. The feature tractor produces a  $2048 \times 1$  size feature vector per sequence. This is the input to train the ReID classifier. During the testing phase, we use the 2048 dimensional feature to measure distance between the test sequence and the sequence from the gallery. We use the Cumulative Matching Characteristic(CMC) and Mean Average Precision(mAP) to evaluate the performance. CMC represents the matching characteristics of the first  $n$  query results.

**Settings.** The network feature extractors have been pre-trained on ImagNet dataset. We follow common data augmentation such as random flips and random crops during training. We use ADAM optimizer to train our model with a batch size of 32. We use a sequence length of 4 to train our model. The flow guided attention has been applied at layer 4 of the ResNet50 and an empirical study of attention at different layers has been presented in the next section. Hence the training setting have mostly been kept similar to our baselines [16]. In order to explore the advantage of attention with optical flow, we propose a separate experimental setup with simple gated attention mechanism i.e using optical flow to attend to image stream alone. This is a one stream approach where only image features are used for classification while optical flow is just used as an attention mechanism as described below.

Given input images,  $I_c^1, I_c^2, \dots, I_c^n$  and flow maps  $F_c^1, F_c^2, \dots, F_c^n$  for images of a sequence, we extract the features  $\phi_c = (\phi_c^1, \phi_c^2, \dots, \phi_c^n)$  and  $f_c = (f_c^1, f_c^2, \dots, f_c^n)$  from the deep CNN and the Flow CNN respectively. A shallow CNN (Flow CNN) has been used to extract features from optical flow maps. We rely on shallow CNN to retain spatial coherence in the flow features (see Fig. 4).

Let  $l$  be the intermediate layer of the  $k$  layer deep CNN and let the deep CNN be represented by  $H$  with a total number of  $k$  layers. Let  $S$  denote the shallow flow feature extractor CNN with  $t = 1, 2, 3 \dots n$  then,

$$\phi_c^t = H(I_c^t), \quad f_c^t = S(F_c^t) \quad (9)$$

If features from layer  $l$  are expressed as  $\psi$ , then

$$\psi_c^t = H_l(I_c^t) \quad (10)$$

The features from Eq. 10 are then pooled in the channel dimension to produce  $N \times 1 \times I \times J$  feature for attention in the spatial dimension. The features are then activated by an activation function to produce a spatial soft attention map  $\text{map}(A(f_c^t))$ , where  $A$  is the sigmoid activation function, and  $a_c^t$  is the output of the activation function. Finally attention is applied to the intermediate features  $\psi$  at an intermediate layer to obtain activated features  $\Psi$  by element-wise multiplication with the activation  $a_c^t$ .

$$\Psi_c^t = \psi_c^t \odot a_c^t \quad (11)$$

After gated attention of features at the intermediate CNN layers, the feature extraction process is continued with the rest of the CNN layers. In Eq. 12  $l, k$  represents layers between intermediate layer  $l$  and last layer  $k$ . Then, the output  $\phi_c^t$  of feature extraction is given by,

$$\phi_c^t = H_{l,k}(\Psi_c^t) \quad (12)$$

$\phi_c^t$  is further average pooled in temporal dimension to produce CNN features for re-identification. The network is trained with classification layer similar to our Mutual Attention Network. The Gated Attention method” described here served as one of the baselines for flow guided attention.

## 5. Results and Discussion

We start this section with some ablation study on contribution of different modules for the final result. We also include some empirical study on selecting the Deep Feature Extractor layer for for attention as well as sequence length selection. We then proceed to overall performance comparison with the baselines and finally a comparison with state-of-the-art-methods. We do the ablation study on baseline ResNet50 architecture based system [16] with temporal pooling for feature aggregation on MARS dataset. We



compare the overall performance on both MARS and Duke-MTMC dataset.

**a) Flow Guided Attention Fusion.** The first part of our work consists of flow guided attention on the intermediate layer of the Deep CNN used for feature extraction in ReID. Different layers in the Deep CNN have different abstraction level of salient features of the input person image. Hence an experiment was conducted by fusing the flow guided attention at different layers of the Deep CNN applied on the baseline [16] ReID system and evaluated on MARS dataset. From the Tab. 1 we conclude that the best performance was achieved by attending at layer 4 of the ResNet50 network. This is justifiable from the fact that the earlier layers have different abstraction level of the salient features, the abstraction level increases in the deeper layers but in the last layer the spatial coherence is lower than the previous layers.

**b) Contribution of Different Modules to the Baseline.** In this subsection we compare Mutual Attention methods to the baseline [16] since we follow similar overall system architecture. In Tab. 2 we compare the baseline and ours with different feature aggregation methods like Average Pooling, Temporal Attention and our weighted feature addition method described earlier. We also compare our

Table 1. Accuracy of our Baseline (ResNet50 + Temporal Pooling, TP) and ou Baseline + Mutual Attention(MA) + TP (Ours) at different layers of ResNet50 on MARS dataset.

Method	maP	Rank-1
Baseline [16]	75.8	83.1
Baseline+MA (Layer2)	78.2	84.5
Baseline+MA (Layer3)	78.8	84.9
Baseline+MA (Layer4)	<b>80.0</b>	<b>86.6</b>
Baseline+MA (Layer5)	78.1	84.3

Table 2. An ablation study of contribution of different module i.e Gated Attention(ours) and our Mutual Attention on the baselines. This study was done on MARS dataset

Method	Feat Aggregation	mAP	Rank 1
Baseline [16] (One Stream)	Pooling	75.8	83.1
No Attention (Two Stream)	Pooling	76.7	84.3
Gated Attention (One Stream)	Pooling	77.4	84.6
Mutual Attention (Two Stream)	Pooling	79.1	85.4
Baseline [16]	RNN	75.7	82.9
Baseline [16]	Temporal Attention	76.7	83.3
Mutual Attention (Mutual Atten)	Weighted Addition	<b>80.0</b>	<b>86.6</b>

Table 3. Empirical study of video sequence length vs performance of our proposed Mutual Attention (MA), and baselines with no attention, average pooling and with RNN on MARS dataset.

No of frames per Sequence	Baseline [16]		RNN Aggreg		Ours		Ours	
	Average Pooling No Attention				Gated Attention Weighted Addition.		Mutual Attention Weighted Addition.	
	MAP	Rank 1	mAP	Rank 1	mAP	Rank 1	mAP	Rank 1
2	71.0	81.8	-	-	77.0	84.0	74.8	82.4
4	75.1	83.2	75.7	82.9	77.8	84.8	77.7	85.4
6	74.4	82.7	-	-	77.6	84.5	79.2	85.8
8	73.3	82.0	76.2	82.5	77.3	84.2	79.3	86.4
16	-	-			72.5	82.9	<b>80.0</b>	<b>86.6</b>

Mutual Attention method with single stream with Gated Attention using optical flow described in the introduction to Experiments section. We can see that just Gated Attention on its own on the baseline [16] has improved the performances by a large margin on MARS datasets. Our Mutual Attention method further improved the results compared to Gated Attention showing the potential of Mutual Attention between both image and optical flow features. Out Feature addition method used with Mutual Attention improve the results for feature aggregation by a larger margin compared to both Average Pooling and aggregation method from Gated Attention.

**c) Effect of Sequence Length.** The length of the sequence has an effect on the representative power of final aggregated feature. This in-turn influences the performance of various feature aggregation methods. Therefore in this subsection we analyse the effect of sequence length on different feature aggregation methods such as Temporal Pooling, Flow guided weighted Addition applied on our method. Hence in Tab. 3 we have shown results of flow guided attention on ResNet50 architecture with both the feature aggregation methods. It can be seen that at the sequence length of 4 we obtain ideal results for most methods in the literature as well as for the simple gated attention method. But our Mutual Attention method demonstrate the ability to aggregate additional features and hence we could use a sequence of length 16 with Mutual Attention. This is a crucial result as we demonstrate ability to aggregate additional features and keep improving results until a sequence length of 16. Longer sequences have attributed to long term better motion and appearance features. At the same time in other methods in literature, simple averaging adds additional noise to the features with longer sequences. Our weighted addition methods weights the individual feature based on importance and relevance thereby reducing noise with longer sequences.

**d) Comparison with State-of-the-Art.** We report the performance of our method with backbones ResNet50 and SE-ResNet50 [21] separately with our Mutual Attention and weighted feature aggregation method on MARS , Duke-MTMC datasets and ILIDS-VID [51] in the Tab. 4 and Tab. 5 compared with related works. As mentioned earlier we have selected [16] as our baseline. It can be observed

Table 4. Accuracy of our proposed method vs state-of-the-art evaluated on MARS and Duke-MTMC dataset.\* next to the method indicates use of optical flow as one of the streams of input.

Method	Reference	MARS		Duke-MTMC	
		mAP	Rank-1	mAP	Rank-1
LOMO+SQDA [26]	CVPR-2015	16.4	30.7	-	-
Set2set [29]	CVPR-2017	51.7	73.7	-	-
JST RNN [60]	CVPR-2017	50.7	70.6	-	-
k-reciprocal [59]	CVPR-2017	58.0	67.8	-	-
TriNet [18]	ArXiv	67.7	79.8	-	-
RQEN [?]	AAAI-2018	71.14	<b>77.83</b>	-	-
Part-Alignment [46]	ECCV-2018	72.2	83.0	78.34	83.62
Mask-Guided [40]	CVPR-2018	71.1	77.1	-	-
Snippet* [6]	CVPR-2018	71.1	82.1	-	-
STA [15]	AAAI-2019	80.8	86.3	94.9	96.2
RevstTempool [16]	Arxiv	75.8	83.1	-	-
Cosam-ResNet50 [44]	ICCV-2019	76.9	83.6	93.5	93.7
STAL [7]	IEEE Transaction	73.5	82.2	-	-
Cosam-SE-ResNet50 [44]	ICCV-2019	79.9	84.9	94.1	95.4
STAR* [52]	BMVC-2019	76.0	85.4	-	-
SCAN [55]	IEEE Transaction	76.7	86.6	-	-
SCAN [55]	IEEE Transaction	77.2	<b>87.2</b>	-	-
Rec3D [8]	IEEE Transaction	80.4	86.3	-	-
GLTR [24]	CVPR 2019	78.47	87.02	93.74	96.29
Mutual Attention(Ours) ResNet-50	<b>Ours</b>	<b>80.0</b>	86.6	94.9	95.6
Mutual Attention(Ours) SE-ResNet-50	<b>Ours</b>	<b>80.9</b>	<b>87.3</b>	94.8	<b>96.7</b>

Table 5. Comparison of the performance of our work with state-of-the-art methods evaluated on ILIDS-Vid dataset.

Method	Reference	Rank 1	Rank 5
Two Stream* [12]	ICCV 2017	60.0	86.0
Snippet [6]	CVPR-2018	85.4	87.8
RQEN [41]	AAAI-2018	77.1	93.2
STAL [41]	IEEE Trans	82.8	95.3
COSAM SE-ResNet50 [44]	ICCV-2019	79.6	95.3
GLTR [24]	CVPR-2019	86.0	-
Rec3D [8]	IEEE Trans	87.9	98.6
Mutual Attention ResNet-50	Ours	86.2	96.4
Mutual Attention SE ResNet-50	Ours	<b>88.1</b>	98.4

that from our baseline. we have improved by a large margin on both mAP and Rank1 metric. Our method has also outperformed most of the state-of-the-art methods including some of the best existing methods. We have also shown the advantage of our method compared to other optical flow based methods [55, 52, 6]. Although [27] have demonstrated State-Of-the-Art results, we do not compare with them as their evaluation strategy is different from that of the commonly followed method in literature. We attribute our performance gain compared to the baseline on both flow guided attention and our feature aggregation technique. It can also be observed that from our proposal Mutual Atten-

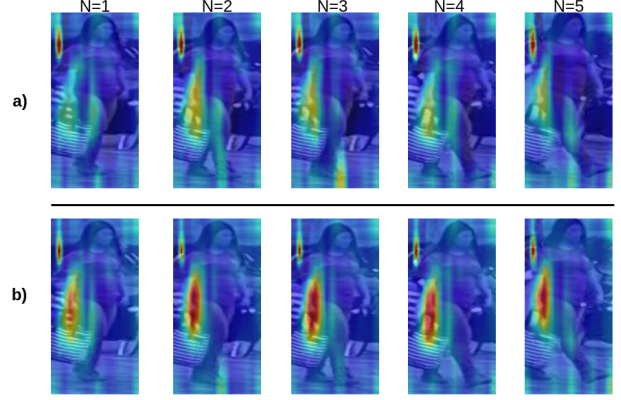


Figure 5. Visualization of feature maps produced using a 5-image video clip selected from the MARS dataset. The video clip on the top row (a) shows the activations of the feature maps without any attention, while the bottom row shows (b) the activations of feature maps with flow guided attention.

tion method performs best demonstrating that optical flow and image stream can attend to the salient regions of each other. Our proposed Mutual Attention method could be integrated with any back-end architecture from some of the strong baselines to achieve better performance. Since our main aim was to evaluate the contribution of Mutual Attention clearly, we choose a simple baseline [16]. Compared to the results on other datasets, the margin of improvement is higher with ILIDS-VID dataset due to uniformly centered hand-annotated person cutouts of ILIDS-VID dataset. Results also suggest that our proposed approach is vulnerable to quality of person detection and tracking.

**d) Visualization.** Fig. 5 shows activations of feature maps from final layer of our backbone 2D-CNN feature extractor. The top row (a) shows activations without any attention, and the bottom row (b) shows the activations after flow guided attention. It can be observed that our flow guided attention has enhanced the spatial activations of feature maps based on the optical flow produced by the virtue of motion of the person between different frame of the sequence.

## 6. Conclusion

In this work we present a novel framework for flow guided attention and temporal feature aggregation for Person-ReID. The sole purpose of the work has been to focus on visual appearances across spatial and temporal streams and their correlations to encode common saliency between the streams, reduce background clutter, learn motion patterns of person and to have the advantages of having longer sequences. Our feature aggregation method uses cues from both image and optical flow feature to assign weights and aggregate image instance features to produce a single video feature representation unlike assigning equal weights to images instances as in temporal pooling. Our method outperforms the state-of-the-art person reID meth-



ods in terms of both mAP and Rank1 accuracy evaluated on MARS, Duke-MTMC, and ILIDS-VID datasets. The proposed Mutual Attention network is most effective when the person detection and tracking produces high quality bounding-boxes, and in scenarios with bigger-sized bounding boxes for objects, where the attention helps in locating the objects.

## References

- [1] Ejaz Ahmed, Michael Jones, and Tim K Marks. An improved deep learning architecture for person re-identification. In *CVPR*, 2015.
- [2] Amran Bhuiyan, Yang Liu, Parthipan Siva, Mehrrsan Javan, Ismail Ben Ayed, and Eric Granger. Pose guided gated fusion for person re-identification. In *WACV*, 2020.
- [3] Amran Bhuiyan, Alessandro Perina, and Vittorio Murino. Person re-identification by discriminatively selecting parts and features. In *ECCV*, 2014.
- [4] Amran Bhuiyan, Alessandro Perina, and Vittorio Murino. Exploiting multiple detections for person re-identification. *Journal of Imaging*, 4(2):28, 2018.
- [5] Jane Bromley, Isabelle Guyon, Yann LeCun, Eduard Säckinger, and Roopak Shah. Signature verification using a “siamese” time delay neural network. In *NIPS*, 1994.
- [6] D. Chen, H. Li, T. Xiao, S. Yi, and X. Wang. Video person re-identification with competitive snippet-similarity aggregation and co-attentive snippet embedding. In *ICCV*, pages 1169–1178, June 2018.
- [7] Guangyi Chen, Jiwen Lu, Ming Yang, and Jie Zhou. Spatial-temporal attention-aware learning for video-based person re-identification. *IEEE Transactions on Image Processing*, 28(9):4192–4205, 2019.
- [8] Guangyi Chen, Jiwen Lu, Ming Yang, and Jie Zhou. Learning recurrent 3d attention for video-based person re-identification. *IEEE Transactions on Image Processing*, 2020.
- [9] Weihua Chen, Xiaotang Chen, Jianguo Zhang, and Kaiqi Huang. Beyond triplet loss: a deep quadruplet network for person re-identification. In *CVPR*, 2017.
- [10] De Cheng, Yihong Gong, Sanping Zhou, Jinjun Wang, and Nanning Zheng. Person re-identification by multi-channel parts-based cnn with improved triplet loss function. In *CVPR*, 2016.
- [11] Sangwoo Cho and Hassan Foroosh. Spatio-temporal fusion networks for action recognition. In *ACCV*, pages 347–364. Springer, 2018.
- [12] D. Chung, K. Tahboub, and E. J. Delp. A two stream siamese convolutional neural network for person re-identification. In *ICCV*, pages 1992–2000, Oct 2017.
- [13] J. Deng, W. Dong, R. Socher, L.-J. Li, K. Li, and L. Fei-Fei. ImageNet: A Large-Scale Hierarchical Image Database. In *CVPR09*, 2009.
- [14] Michela Farenzena, Loris Bazzani, Alessandro Perina, Vittorio Murino, and Marco Cristani. Person re-identification by symmetry-driven accumulation of local features. In *CVPR*, 2010.
- [15] Yang Fu, Xiaoyang Wang, Yunchao Wei, and Thomas Huang. Sta: Spatial-temporal attention for large-scale video-based person re-identification. In *AAAI 2019*, volume 33, pages 8287–8294, 2019.
- [16] Jiyang Gao and Ram Nevatia. Revisiting temporal modeling for video-based person reid. *arXiv preprint arXiv:1805.02104*, 2018.
- [17] Xinqian Gu, Bingpeng Ma, Hong Chang, Shiguang Shan, and Xilin Chen. Temporal knowledge propagation for image-to-video person re-identification. In *ICCV*, 2019.
- [18] Alexander Hermans, Lucas Beyer, and Bastian Leibe. In defense of the triplet loss for person re-identification. *arXiv preprint arXiv:1703.07737*, 2017.
- [19] Ruibing Hou, Bingpeng Ma, Hong Chang, Xinqian Gu, Shiguang Shan, and Xilin Chen. Vrsc: Occlusion-free video person re-identification. In *CVPR*, June 2019.
- [20] J. Hu, L. Shen, and G. Sun. Squeeze-and-excitation networks. In *CVPR*, pages 7132–7141, June 2018.
- [21] Jie Hu, Li Shen, and Gang Sun. Squeeze-and-excitation networks. In *Proceedings of the IEEE conference on computer vision and pattern recognition*, pages 7132–7141, 2018.
- [22] Tak-Wai Hui, Xiaoou Tang, and Chen Change Loy. Liteflownet: A lightweight convolutional neural network for optical flow estimation. In *CVPR*, pages 8981–8989, 2018.
- [23] Dangwei Li, Xiaotang Chen, Zhang Zhang, and Kaiqi Huang. Learning deep context-aware features over body and latent parts for person re-identification. In *CVPR*, 2017.
- [24] Jianing Li, Jingdong Wang, Qi Tian, Wen Gao, and Shiliang Zhang. Global-local temporal representations for video person re-identification. In *CVPR*, pages 3958–3967, 2019.
- [25] Jianing Li, Shiliang Zhang, and Tiejun Huang. Multi-scale 3d convolution network for video based person re-identification. In *AAAI*, volume 33, pages 8618–8625, 2019.
- [26] Shengcai Liao, Yang Hu, Xiangyu Zhu, and Stan Z Li. Person re-identification by local maximal occurrence representation and metric learning. In *CVPR*, 2015.
- [27] Chih-Ting Liu, Chih-Wei Wu, Yu-Chiang Frank Wang, and Shao-Yi Chien. Spatially and temporally efficient non-local attention network for video-based person re-identification. In *BMVC*, 2019.
- [28] Hao Liu, Jiashi Feng, Meibin Qi, Jianguo Jiang, and Shuicheng Yan. End-to-end comparative attention networks for person re-identification. *IEEE Transactions on Image Processing*, 26(7):3492–3506, 2017.
- [29] Yu Liu, Yan Junjie, and Wanli Ouyang. Quality aware network for set to set recognition. In *CVPR*, 2017.
- [30] Chih-Yao Ma, Min-Hung Chen, Zsolt Kira, and Ghassan AlRegib. Ts- lstm and temporal-inception: Exploiting spatiotemporal dynamics for activity recognition. *Signal Processing: Image Communication*, 71:76–87, 2019.
- [31] N. McLaughlin, J. M. d. Rincon, and P. Miller. Recurrent convolutional network for video-based person re-identification. In *CVPR*, pages 1325–1334, June 2016.
- [32] N. McLaughlin, J. M. d. Rincon, and P. Miller. Recurrent convolutional network for video-based person re-identification. In *CVPR*, pages 1325–1334, June 2016.

- [33] Rameswar Panda, Amran Bhuiyan, Vittorio Murino, and Amit K Roy-Chowdhury. Unsupervised adaptive re-identification in open world dynamic camera networks. In *CVPR*, 2017.
- [34] Xuelin Qian, Yanwei Fu, Tao Xiang, Wenxuan Wang, Jie Qiu, Yang Wu, Yu-Gang Jiang, and Xiangyang Xue. Pose-normalized image generation for person re-identification. In *ECCV*, 2018.
- [35] Ruijie Quan, Xuanyi Dong, Yu Wu, Linchao Zhu, and Yi Yang. Auto-reid: Searching for a part-aware convnet for person re-identification. *ICCV*, 2019.
- [36] Ergys Ristani, Francesco Solera, Roger Zou, Rita Cucchiara, and Carlo Tomasi. Performance measures and a data set for multi-target, multi-camera tracking. In *ECCVWK*, 2016.
- [37] M Saquib Sarfraz, Arne Schumann, Andreas Eberle, and Rainer Stiefelhausen. A pose-sensitive embedding for person re-identification with expanded cross neighborhood re-ranking. In *ICCV*, 2018.
- [38] J. Si, H. Zhang, C. Li, J. Kuen, X. Kong, A. C. Kot, and G. Wang. Dual attention matching network for context-aware feature sequence based person re-identification. In *CVPR*, pages 5363–5372, June 2018.
- [39] Karen Simonyan and Andrew Zisserman. Two-stream convolutional networks for action recognition in videos. In *Advances in neural information processing systems*, pages 568–576, 2014.
- [40] C. Song, Y. Huang, W. Ouyang, and L. Wang. Mask-guided contrastive attention model for person re-identification. In *CVPR*, pages 1179–1188, June 2018.
- [41] Guanglu Song, Biao Leng, Yu Liu, Congrui Hetang, and Shaofan Cai. Region-based quality estimation network for large-scale person re-identification. *arXiv preprint arXiv:1711.08766*, 2017.
- [42] Springer. *MARS: A Video Benchmark for Large-Scale Person Re-identification*, 2016.
- [43] Chi Su, Jianing Li, Shiliang Zhang, Junliang Xing, Wen Gao, and Qi Tian. Pose-driven deep convolutional model for person re-identification. In *ICCV*, 2017.
- [44] Arulkumar Subramaniam, Athira Nambiar, and Anurag Mittal. Co-segmentation inspired attention networks for video-based person re-identification. In *ICCV*, October 2019.
- [45] Yumin Suh, Jingdong Wang, Siyu Tang, Tao Mei, and Kyoung Mu Lee. Part-aligned bilinear representations for person re-identification. *ECCV*, 2018.
- [46] Yumin Suh, Jingdong Wang, Siyu Tang, Tao Mei, and Kyoung Mu Lee. Part-aligned bilinear representations for person re-identification. In *ECCV*, 2018.
- [47] Yifan Sun, Liang Zheng, Yi Yang, Qi Tian, and Shengjin Wang. Beyond part models: Person retrieval with refined part pooling (and a strong convolutional baseline). In *ECCV*, 2018.
- [48] Chiat-Pin Tay, Sharmili Roy, and Kim-Hui Yap. Aanet: Attribute attention network for person re-identifications. In *CVPR*, 2019.
- [49] Pavan Turaga, Rama Chellappa, and Ashok Veeraraghavan. Advances in video-based human activity analysis: Challenges and approaches. In Marvin V. Zelkowitz, editor, *Advances in Computers*, volume 80 of *Advances in Computers*, pages 237 – 290. Elsevier, 2010.
- [50] Rahul Rama Vior, Mrinal Haloi, and Gang Wang. Gated siamese convolutional neural network architecture for human re-identification. In *ECCV*, 2016.
- [51] Taiqing Wang, Shaogang Gong, Xiatian Zhu, and Shengjin Wang. Person re-identification by video ranking. In *ECCV*, pages 688–703. Springer, 2014.
- [52] Guile Wu, Xiatian Zhu, and Shaogang Gong. Tracklet self-supervised learning for unsupervised person re-identification. In *AAAI*, 2020.
- [53] Yu Wu, Yutian Lin, Xuanyi Dong, Yan Yan, Wanli Ouyang, and Yi Yang. Exploit the unknown gradually: One-shot video-based person re-identification by stepwise learning. In *CVPR*, June 2018.
- [54] Dong Yi, Zhen Lei, Shengcai Liao, and Stan Z Li. Deep metric learning for person re-identification. In *ICPR*, 2014.
- [55] Ruimao Zhang, Jingyu Li, Hongbin Sun, Yuying Ge, Ping Luo, Xiaogang Wang, and Liang Lin. Scan: Self-and-collaborative attention network for video person re-identification. *IEEE Transactions on Image Processing*, 28(10):4870–4882, 2019.
- [56] Haiyu Zhao, Maoqing Tian, Shuyang Sun, Jing Shao, Junjie Yan, Shuai Yi, Xiaogang Wang, and Xiaoou Tang. Spindle net: Person re-identification with human body region guided feature decomposition and fusion. In *CVPR*, 2017.
- [57] Liming Zhao, Xi Li, Yueting Zhuang, and Jingdong Wang. Deeply-learned part-aligned representations for person re-identification. In *CVPR*, 2017.
- [58] Liang Zheng, Yujia Huang, Huchuan Lu, and Yi Yang. Pose invariant embedding for deep person re-identification. *arXiv preprint arXiv:1701.07732*, 2017.
- [59] Zhun Zhong, Liang Zheng, Donglin Cao, and Shaozi Li. Re-ranking person re-identification with k-reciprocal encoding. In *CVPR*, 2017.
- [60] Z. Zhou, Y. Huang, W. Wang, L. Wang, and T. Tan. See the forest for the trees: Joint spatial and temporal recurrent neural networks for video-based person re-identification. In *CVPR*, pages 6776–6785, July 2017.